Physical Review B 69, 2004, 155114-1 – 155114-7

Geometric and electronic structure of γ-V_2O_5: Comparison between α-V_2O_5 and γ-V_2O_5

M. Willinger,* N. Pinna,† D. S. Su, and R. Schlögl
Department of Inorganic Chemistry, Fritz-Haber-Institut der Max-Planck-Gesellschaft, Faradayweg 4-6, D-14195 Berlin, Germany
(Received 14 August 2003; revised manuscript received 19 February 2004; published 28 April 2004)

Electronic structure calculations of γ-V_2O_5 are presented and compared to the electronic structure of the more commonly known α-V_2O_5. The different VO_5 building blocks in γ-V_2O_5 are investigated in terms of the angular momentum projected density of states. Since the same structural unit is also found in the α-V_2O_5 phase, it is possible to compare the electronic structure with respect to differences in the geometry of the VO_5 pyramids. Electron energy-loss spectroscopy is applied as a sensitive probe of the electronic structure and reveals differences in the fine structure of the oxygen K ionization edge which are confirmed by the simulation.

I. INTRODUCTION

Vanadium oxides merit special attention because of their outstanding structural flexibility combined with chemical and physical properties which are of interest for catalytic and electrochemical applications. Specially α-V_2O_5 is an essential ingredient to heterogeneous catalysis and its electronic and structural properties have been widely studied.[1–4] γ-V_2O_5 is a polymorph of the most common known α-V_2O_5 phase and was first reported in 1991 by Cocciantelli *et al.* who investigated charging and decharging cycles of LiV_2O_5 batteries.[5] While the electronic behavior of γ-LiV_2O_5 (Ref. 6) has been modeled by means of density-functional theory-(DFT), the electronic structure of γ-V_2O_5 remained untouched. Recently, γ-V_2O_5 attracts new attention since the synthesis of γ-V_2O_5 nanowires and nanorods by the reverse micelle technique opens access to a geometrically well-defined nanosized model catalyst.[7,8] During the synthesis the size and shape of the particles can be controlled by varying the time for which the particles are kept in the micellar solution spanning from hours to days.

The close relation between the geometric structure of α-V_2O_5 and γ-V_2O_5 as well as the possible conversion between the two structures is also of interest in view of a very promising application of V_2O_5 nanofibre sheets as actuators as reported by Gu *et al.*[9] and also in view of the huge efforts in synthesis of one-dimensional anisotropic VO-x nanotubes and nanorods for future nanotechnology.[10,11] The catalytic relevance of the V^{5+} oxidation state combined with the structural peculiarities of the synthesized particles and the close relation to the α-V_2O_5 phase motivates the investigation of the electronic structure of γ-V_2O_5.

This work presents the first investigation of the electronic structure of γ-V_2O_5 and is based on DFT. The aim is to compare the basic structural VO_5 units in γ-V_2O_5 and α-V_2O_5 with respect to differences in their geometric and electronic structure. A detailed understanding of the relation between geometric and electronic structures is essential since this basic structural unit is also common to the industrial VPO catalysts used for n-butane selective oxidation.[12]

Band-structure calculations were performed using the FP-LAPW (full potential linearized augmented plane-wave) method.[13] To compare the theoretical results with experiments, the energy loss near edge structure of the oxygen K ionization edge (O K ELNES) was simulated and compared to spectra recorded from α-V_2O_5 and from γ-V_2O_5 nanorods.

II. GEOMETRIC STRUCTURE

The γ-V_2O_5 forms a layer-type orthorhombic lattice with constants $a=9.946(0)$ Å, $b=3.585(0)$ Å, and $c=10.042(0)$ Å.[5] The structure is set up by layers of edge and corner sharing VO_5 pyramids sticking out at both sides of the layer. As opposed to α-V_2O_5, where all V=O vanadyl bonds are oriented along c (z direction), the double chains of edge sharing pyramids are tilted relatively to each other in γ-V_2O_5 with an angle between the basal plane of the pyramids and the x axis of about $+30°$ and $-30°$, respectively (Fig. 1). Additionally, the VO_5 pyramids are oriented along x as down-up–down-up while in α-V_2O_5 the orientation is down-down–up-up. As a consequence, there exist two structurally different VO_5 pyramids. The first one at the V1 site can also be thought of as a bipyramidal (VO_6) by including the weak interlayer bond to the vanadyl oxygen of the adjacent layer. The second VO_5 pyramid at the V2 site is oriented in such a way that no oxygen atom lies in close vicinity of the basal plane. The existence of the two different vanadium sites has been confirmed by Fourier-transform infrared measurements of γ-V_2O_5 nanorods.[8] Each of the two pyramids contains three structurally different oxygens, but in total, due to the linking via one common oxygen, there exist five different oxygens and two different vanadiums in γ-V_2O_5. The primitive cell comprises four formula units. It is worthwhile to mention here that γ-V_2O_5 undergoes a transformation into the normal form of α-V_2O_5 near 340 °C.[5]

III. CALCULATION AND EXPERIMENTS

Band-structure calculations of the density of states (DOS) were performed using the full potential linear augmented plane-waves code WIEN2K.[13] This package also contains the TELNES program which allows us to simulate electron energy-loss spectra (EELS) by calculating the sum over site and angular momentum projected DOS and DOS cross terms multiplied by the appropriate transition matrix elements.[14]

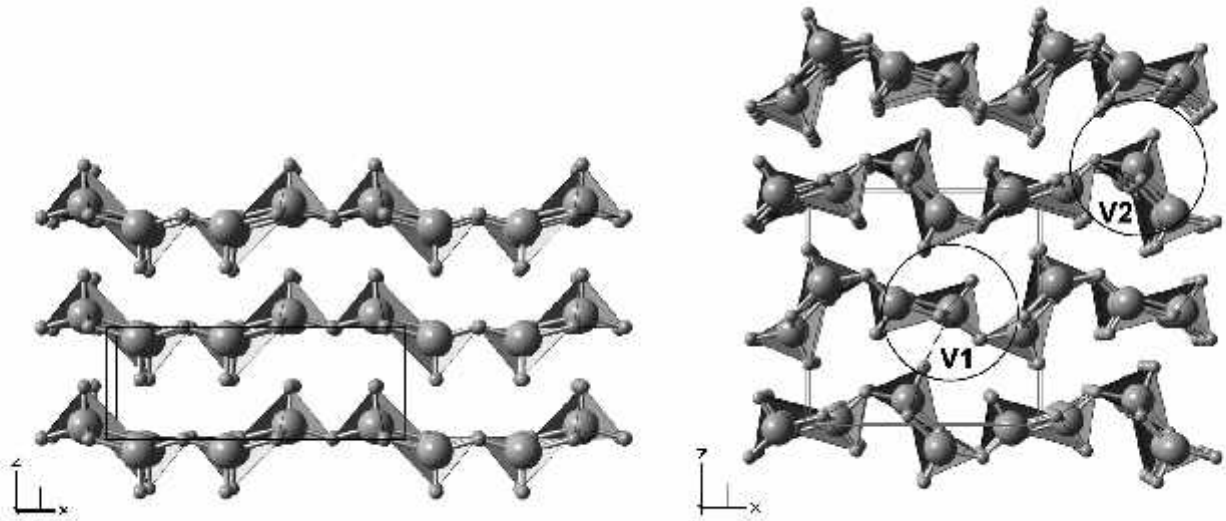

FIG. 1. Crystal structure of α-V_2O_5 and γ-V_2O_5. The orthorhombic unit cells are indicated; a, b, and c are parallel to x, y, and z, respectively. Circles labeled V1 and V2 highlight the two differently surrounded vanadium sites existing in γ-V_2O_5.

Simple unit cells were used for the calculations, and three-dimensional periodic boundary conditions ensure that the space-group symmetry is included properly in the calculation. For γ-V_2O_5 56 k points in the irreducible part of the Brillouin zone and a plane-wave cutoff R_{kmax} of 7.5 (corresponding to an energy cutoff of 28.7 Ry) was used. α-V_2O_5 was calculated with 84 k points and a plane-wave cutoff of 8 (31 Ry). The generalized gradient approximation was used for the exchange-correlation potential.[15] In order to get a good basis set for the projection of the DOS onto p and d states in the simulation, the local coordinates at each atom of the tilted VO_5 pyramids were chosen such that the z axis coincides with the direction of the V=O vanadyl bond. The γ-V_2O_5 nanorods used for the EELS measurements were synthesized using the reverse micelle technique.[7] α-V_2O_5 samples were obtained form Fluka Chemie GmbH. All measurements were performed with a Philips CM 200 field-emission transmission electron microscope equipped with a Gatan energy filter for EELS measurements. The microscope was operated at 200 kV. The energy resolution, estimated from the full width at half maximum of the zero-loss peak, was 1 eV. The EELS spectra of the nanorods sample were recorded at a collection angle of 9.8 mrad and for a large number of nanorods in order to minimize irradiation effects, and with an incident beam perpendicular to the long axis of the nanorods (corresponding to the b axis). The spectra of α-V_2O_5 were recorded with the incident beam parallel to the crystal c axis. In order to average out anisotropic effects the spectrometer acceptance angle was as large as β=9.8 mrad and the beam convergence angle was α=1.5 mrad.[16]

IV. RESULTS AND DISCUSSION

A. Band structure and density of states: γ-V_2O_5

In Fig. 2 the band structure calculated along selected high-symmetry lines within the first Brillouin zone corresponding to the primitive orthorhombic lattice is presented. It shows that the dispersion is strongly energy dependent and reveals bands of small and large dispersion depending on the energy interval in all the symmetry directions. In the valence band, along the direction Γ-X (i.e., parallel to the x axis) the dispersion of the bands is small and the electrons are well localized, while along the Γ-Y direction (i.e., parallel to the y axis) the dispersion measures about 0.5 eV. Along the direction Γ-Z the dispersion is also weak, reflecting the localization of the electrons in the layered structure. In the conduction band the dispersion of the bands along Γ-X and Γ-Z starts to increase at about 5 eV above the Fermi level,

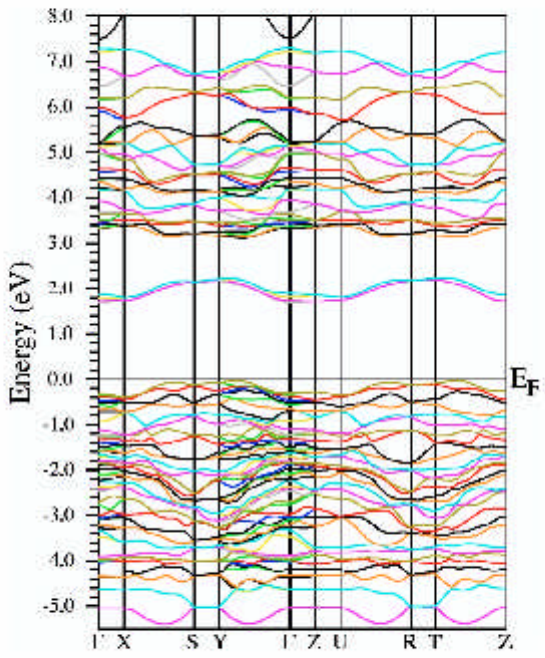

FIG. 2. Band structure of γ-V_2O_5 along symmetry lines within the first Brillouin zone of the simple orthothombic lattice. Energies are given relative to the Fermi level.

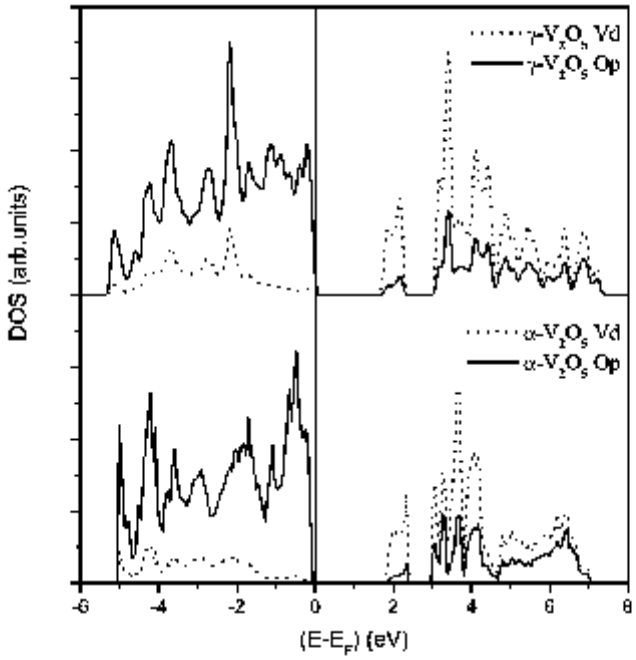

FIG. 3. V 3*d* and O 2*p* projected density of states of α-V_2O_5 and γ-V_2O_5.

whereas the density of the bands decreases. A remarkable feature in the band-structure plot is the split-off conduction band at around 2 eV.

Insight into the chemical and physical properties is gained by observing the vanadium *d* states and their hybridization with the ligand *p* orbitals. The oxygen 2*p* and vanadium 3*d* density of states (Fig. 3) of γ-V_2O_5 and α-V_2O_5 attest the close relation between the structure of the two compounds since the DOS of γ-V_2O_5 exhibits features very similar to the one of α-V_2O_5 (Fig. 3). Both compounds are semiconductors: after a band gap of only 1.70 eV (1.75 eV in α-V_2O_5) a narrow split-off conduction band of 0.6 eV width is separated by another gap of 0.7 eV from the main conduction band. Shape and width of the split-off conduction band are nearly identical for the two polymorph and the separation to the main conduction band is only around 0.1 eV larger in the γ phase. Similar to α-V_2O_5, the valence band of γ-V_2O_5 consists mainly of oxygen 2*p* states with only a small contribution from vanadium 3*d* states, whereas the conduction band mainly comprises the unoccupied vanadium 3*d* states. Common features in the oxygen and vanadium DOS are observed for both compounds and reflect a substantial degree of

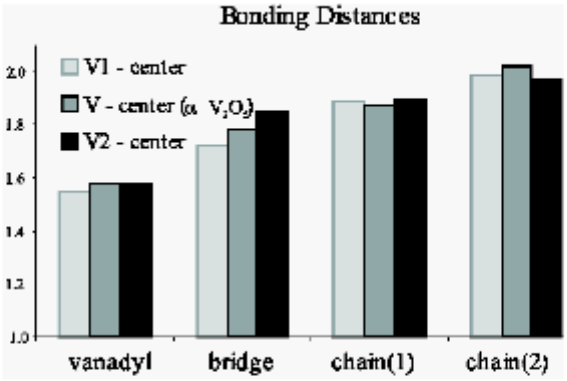

FIG. 5. Comparison of the bonding length at the different V sites.

hybridization between oxygen 2*p* and vanadium 3*d* states. This hybridization has extensively been discussed by Eyert and Höck[3] for the case of α-V_2O_5.

In the following, differences in the VO_5 building blocks will be considered in the discussion of the DOS.

B. Comparison of the different VO_5 units in γ-V_2O_5 and α-V_2O_5

A characteristic of the γ-V_2O_5 structure is the existence of two different sites for the vanadium atoms. The basic structural units in γ-V_2O_5 and α-V_2O_5 are distorted VO_5 pyramids (see Fig. 4). These pyramids have similar features: one short bond to the vanadyl oxygen, one bond to a bridging oxygen linking two pyramids at a pyramid corner, and three bonds to chain oxygens, of which two have the same bonding distance to the vanadium center. However, the interatomic distances are different and from the dispersion of the V-O bonding distances in the pyramid base follows that the distortion at the V1 site is bigger than in the case of α-V_2O_5. At the V2 site, on the other hand, the distortion is less than in α-V_2O_5. The bonding distances in γ-V_2O_5 and α-V_2O_5 are compared against each other in Fig. 5.

The distance from the vanadium center to a vanadyl oxygen from the adjacent plane measures 2.793 Å for α-V_2O_5 and 2.714 Å at the V1 site in γ-V_2O_5. Taking the weak interlayer bond into account results in a sixfold coordinated vanadium. The crystal-field splitting is determined by the geometry of the surrounding oxygen atoms and leads to a separation of the lower part of the conduction band. States forming π^* antibonds appear at lower energy whereas σ^*

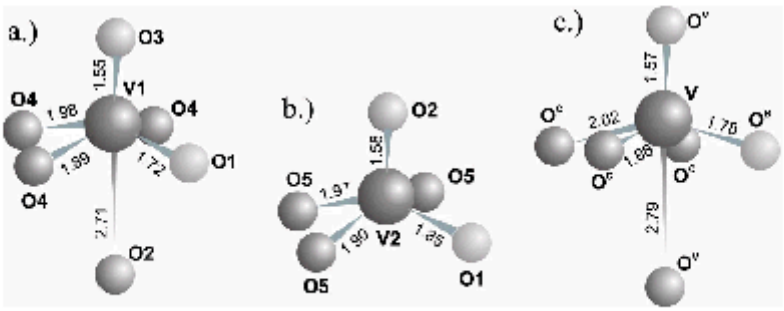

FIG. 4. Local surrounding at the different vanadium sites in γ-V_2O_5 [V1 (a) and V2 (b)] and in α-V_2O_5 (c). The oxygen atoms are labeled as O3, O2, O^V—vanadyl oxygen; O4, O5, O^C—chain oxygen; O1 and O^B—bridge oxygen.

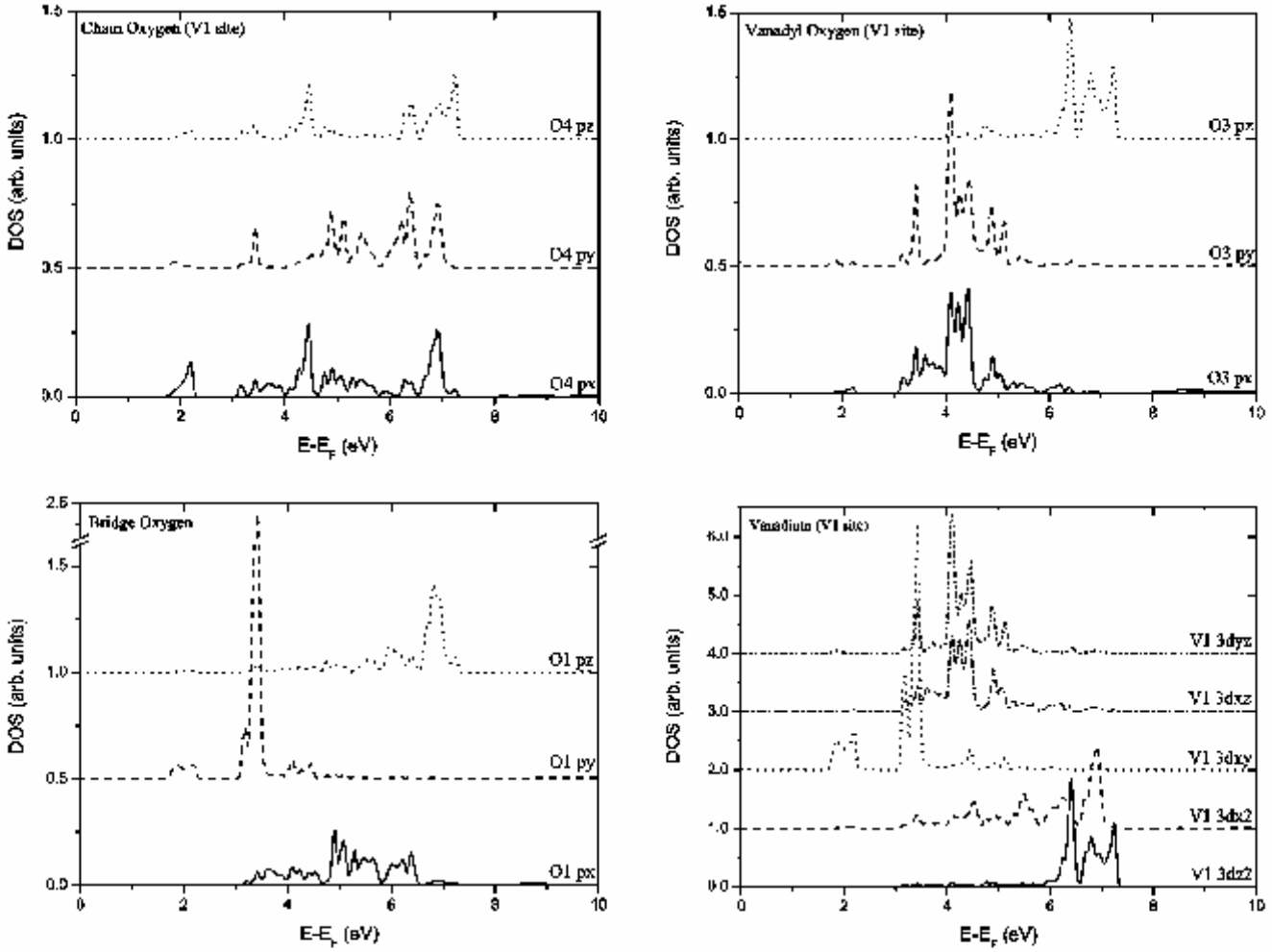

FIG. 6. Angular momentum projected DOS at the V1 site.

antibonds are formed at higher energy. The two subgroups of the unoccupied orbitals are separated by a ligand field splitting. The angular momentum projected DOS's (PDOS's) are presented in Figs. 6 and 7 for the two vanadium sites and their oxygen ligands.

Due to the choice of the local coordinate system at each atom of the tilted pyramids, the $3d$ DOS is projected onto the different orbitals such that the vanadium $3d_{z^2-y^2}$ orbitals point towards the vanadyl oxygen and the $3d_{x^2-y^2}$ orbitals point in the direction of the three chain oxygens and the bridging oxygen. Consequently these two orbitals form σ^* antibonding combinations with the oxygen $2p$ orbitals and appear in the upper region of the lower conduction band. At the V1 site the $3d_{z^2-y^2}$ orbital provides a narrow contribution to the DOS between 6 and 7.5 eV which is identically mirrored by the vanadyl oxygen $2p_z$ orbital. The same agreement in the DOS of the $3d_{z^2-y^2}$ orbital and the vanadyl oxygen $2p_z$ orbital of the V2 site is observed in the energy range between about 4.5 and 6.5 eV. Due to the fact that the vanadium atoms are not in plane with the chain and bridge oxygens, the contribution of the $3d_{x^2-y^2}$ orbitals reaches into the π^* region. At lower energies, the vanadium $3d_{xz}$ and $3d_{yz}$ orbitals mainly combine with the vanadyl oxygen $2p_x$ and $2p_y$ orbitals by forming π^* states. Consequently, the features between around 2 and 7 eV at the V1 and between around 2 and 6 eV at the V2 center are reproduced by the respective vanadyl oxygen $2p_x$ and $2p_y$ orbitals. The remaining vanadium $3d_{xy}$ orbital lies lowest in energy and stretches in between the chain and the bridge oxygens, forming π^* combinations. At the V1 site, it forms a strong and very localized combination with the bridging O1 $2p_y$ orbital between 3 and 4 eV. Although the distance between the bridging oxygen and the V2 center is only slightly larger, the degree of hybridization between the V2 $3d_{xy}$ and the O1 $2p_y$ orbital is much smaller. Instead the V2 $3d_{xy}$ orbital provides the main contribution to the split-off conduction band by forming π^* combinations mainly with the chain oxygen (O5) $2p_x$, $2p_y$ and the bridge (O1) $2p_y$ orbital. In fact it is an interesting consequence of the different geometry of the V1 and V2 pyramids that the intensity of the two features in the respective $3d_{xy}$ DOS is reverse. For the V1 site (Fig. 6) and in the α phase,[3] where the vanadium atom is formally sixfold coordinated in a distorted octahedron, the crystal-field splitting is well developed and clearly separates in energy π^* from σ^* forming states. The splitting is best represented in the DOS of the vanadyl oxygen (O3) $2p$ orbitals

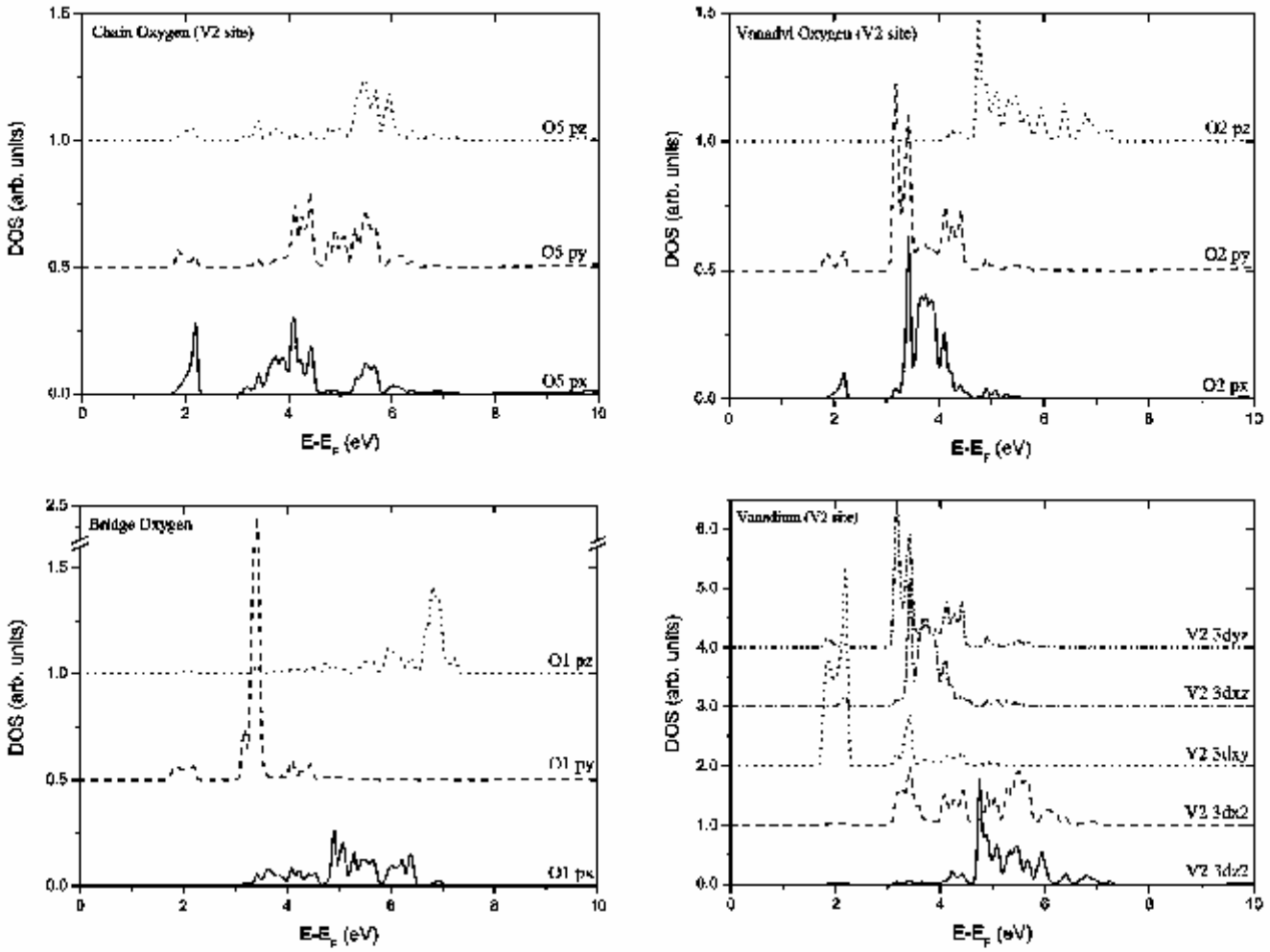

FIG. 7. Angular momentum projected DOS at the V2 site.

which form clear π^* and σ^* states. It measures around 2.6 eV (estimated form the separation of the center of mass of the unoccupied O3 $2p$ states). At the fivefold coordinated V2 site the difference between the longest and the shortest V—O distance is smaller and the resulting pyramid is less distorted. This is reflected in the $2p$ projected DOS of the vanadyl oxygen (O2) at the V2 site where the π^* and σ^* forming states lie closer in energy and the separation of the center of mass measures only around 1.8 eV (see Fig. 7).

Interlayer coupling leads to similarities in the V1 and O2 PDOSs. A comparison reveals only a slight agreement in the O2 $2p_z$ and V1 $3d_{z^2-r^2}$ PDOS's at around 7 eV above the Fermi level. The existence of a small hybridization comes apparent from a comparison of the width of the O3 and O2 $2p_z$ PDOS's: the broadening of the latter is caused by interaction with the V1 $3d_{z^2-r^2}$ orbital. Nevertheless, the agreement is small and underlines the fact that the interlayer bonding is weak and that the picture of the fivefold coordinated pyramid is more accurate than the octahedral description. In α-V_2O_5 there exists only one kind of vanadyl oxygen and therefore it is not possible to separate out information from the PDOS about the orbital overlap between the layers. Nevertheless, single-layer SLAB calculations of Chakrabarti *et al.*[2] demonstrate a weak electronic interlayer coupling also in α-V_2O_5. The role of the vanadyl oxygen from the adjacent layer can therefore be neglected and the stronger crystal-field splitting at the V1 results from the higher distortion of the VO_5 pyramid.

C. ELNES: Simulation and experiment

EELS is applied to probe the local electronic structure and the oxidation state of vanadium in γ-V_2O_5.

The shape of the vanadium and oxygen edges is strongly related to the oxidation state of the vanadium and to the distortion of the coordination polyhedra.[17] In particular, the vanadium white line ratio reacts very sensitively to the oxidation state.[18,19] In α-V_2O_5, the VL_{II} edge is more intense than the VL_{III} edge[20] (Fig. 8 bottom), whereas, with decreasing oxidation state, the VL_{II} intensity decreases relative to the L_{III} spectral weight. This fingerprint allows a reliable assignment of the oxidation state of the vanadium. For this reason also the vanadium white lines are presented, although the following discussion as well as the simulation is based on the O K edge. The focus on the O K edge is justified by the fact that within a one-electron approximation the

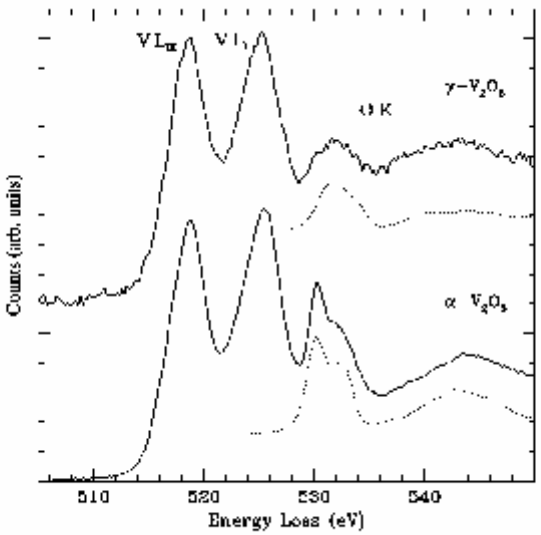

FIG. 8. EELS spectra of α-V_2O_5 (bottom) and of γ-V_2O_5 nanorods (top) for the vanadium $2p$ and the oxygen $1s$. Calculations of the oxygen edge (dotted lines).

simulation of the $2p$ to $3d$ transition giving rise to the L edge fails due to strong electron correlation effects.[21] In α-V_2O_5, the OK edge is characterized by a fine structure (Fig. 8) at around 530 eV exhibiting two contributions arising from transitions from an O $1s$ state to a final $2p$ state in π^* or in σ^* hybridization with a vanadium $3d$ state. *Ab initio* band-structure calculations combined with the simulation of spectra with the TELNES program support the interpretation of the near-edge fine structure in EELS and allow us to directly assign features to the corresponding transitions. Figure 8 demonstrates the close agreement between simulation and experiment, although the core hole left by the excited electron and the high-energy tail of the preceding VL_{II} edge were not taken into account in the simulation.

In the spectra of γ-V_2O_5, the vanadium VL_{II} peak is more intense than the VL_{III} indicating an oxidation state of +5 for vanadium.[19] The shape of the OK feature centered at 531.6 eV is quite different to the one observed for α-V_2O_5 and consists of a single-asymmetric peak centered at around 532 eV and a broad peak at around 544 eV. The calculations for γ-V_2O_5 (dotted line in Fig. 8) agree very well with the experimental data. The close agreement with the bulk simulation also confirms the weak interlayer interaction as the size and surface effects of the γ-V_2O_5 nanorods have negligible effect on the ELNES. Simulation and experiment show that the fine structure visible in the OK edge of α-V_2O_5 has vanished. An explanation follows from a closer observation of the two different vanadium surroundings present in γ-V_2O_5. Five differently coordinated oxygen atoms contribute to the spectrum and the total OK spectral weight is the sum of these contributions, of which each has its individual shape. As a result the π^* and σ^* components overlap and are no longer distinguishable in the total OK edge. In Fig. 9 the single contributions of the different oxygens to the ELNES are presented. When the contributions of the corresponding oxygens surrounding the V1 and V2 centers are added up, the representative ELNES of the two pyramids are obtained (Fig. 9 right). Knowing that the interlayer bond is very weak and can be neglected in this respect, one ends up comparing three differently distorted VO_5 pyramids (at the V1 and V2 sites and in the α phase). The separation between the π^* and σ^* states are visible in the calculated ELNES of the V1 pyramid whereas this separation is no more observable at the V2 site. This underlines the similarity between the VO_5 pyramid at the V1 site and the pyramid of the α phase.

V. CONCLUSION

The theoretical investigation of the band structure and density of states of different VO_5 building blocks in γ-V_2O_5 and α-V_2O_5 gives insight into the relation between geometric and electronic structure. The general distribution of features such as the split-off conduction band and the width of band gaps in the oxygen and vanadium DOS of the two compounds attest the close agreement between the two struc-

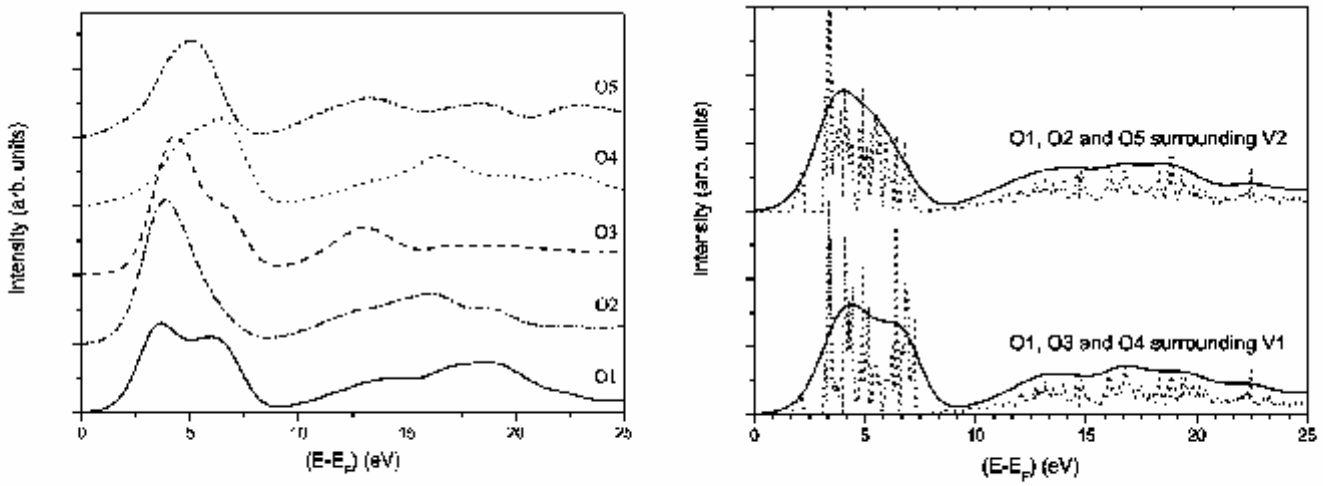

FIG. 9. Single contributions of the different oxygens to the OK ELNES (left) and sum over oxygen contributions arising from VO_5 pyramids at the V1 and V2 sites (with and without experimental broadening) (right).

tures. However, the angular momentum projected DOS reveals a splitting of the vanadium d states into π^* and σ^* forming states which is very sensitive to the geometry of the O ligands. At the V1 site, where the distortion of the VO_5 pyramid, measured from the dispersion of the bonding distances is largest, the splitting is well pronounced. At the V2 site the distortion is smaller and the π^* and σ^* regions show a slight overlap. The splitting at each site is best reproduced by the respective vanadyl oxygen $2p$ orbitals. A detailed investigation of the angular momentum projected DOS reveals that the distribution of intensities in the DOS acts very sensitively on small changes in the bonding distance and geometry. The determined difference in electronic structure of the two polymorph results solely from their different geometric structure. Differences in the electronic structure combined with a fixed chemical composition allow, in a further step, us to elucidate a correlation between the DOS and relevant chemical properties, such as catalytic performance. From this information one can then draw back conclusions about electronic properties relevant for a specific catalytic process.

From a comparison of similar features in the DOS of V1 and the vanadyl oxygen of the adjacent layer (O2) it could be concluded that the interlayer coupling is indeed very weak and that the picture of a distorted pyramidal surrounding has to be favored with respect to a distorted octahedral description. The close agreement between simulated and measured OK ELNES supports the interpretation of the changing in the fine structure of the OK edge between the α and γ phases. With respect to the catalytic potential of α-V_2O_5 it is of relevance to compare and further investigate the two polymorph of the same chemical composition with known differences in the electronic properties. They allow us to probe the concept of structure-activity correlation in a rigorous manner. However, this is beyond the scope of the present paper.

ACKNOWLEDGMENTS

This work was supported by Grant No. SFB 546 of the Deutsche Forschungsgemeinschaft. The authors would like to thank C. Hébert, P. Schattschneider, and W.-D. Schöne for helpful discussions.

*Electronic address: marc@fhi-berlin.mpg.de
†Electronic address: pinna@mpikg-golm.mpg.de

[1] M. Witko, R. Tokarz, and J. Haber, Appl. Catal., A **157**, 23 (1997).
[2] A. Chakrabarti, K. Hermann, R. Druzinic, M. Witko, F. Wagner, and M. Petersen, Phys. Rev. B **59**, 10 583 (1999).
[3] V. Eyert and K.-H. Höck, Phys. Rev. B **57**, 12 727 (1998).
[4] S. Atzkern, S.V. Borisenko, M. Knupfer, M.S. Golden, and J. Fink, Phys. Rev. B **61**, 12 792 (2000).
[5] J.M. Cocciantelli, P. Gravereau, J.P. Doumerc, M. Pouchard, and P. Hagenmuller, J. Solid State Chem. **93**, 497 (1991).
[6] R. Valenti, T. Saha-Dasgupta, J.V. Alvarez, K. Požgajčić, and C. Gros, Phys. Rev. Lett. **86**, 5381 (2001).
[7] N. Pinna, U. Wild, J. Urban, and R. Schlögl, Adv. Mater. (Weinheim, Ger.) **15**, 329 (2003).
[8] N. Pinna, M. Willinger, K. Weiss, J. Urban, and R. Schlögl, Nano Lett. **3**, 1131 (2003).
[9] G. Gu, M. Schmid, P. Chiu, A. Minett, J. Fraysse, G. Kim, S. Roth, M. Kozlov, E. Munoz, and R.H. Baughman, Nat. Mater. **2**, 316 (2003).
[10] G.R. Patzke, F. Krumreich, and R. Nesper, Angew. Chem., Int. Ed. **41**, 2446 (2002).
[11] V.V. Ivanovskaya, A.N. Enyashin, A.A. Sofronov, Yu.N. Makurin, and N.I. Medvedeva, and A.L. Ivanovskii, Solid State Commun. **126**, 489 (2003).
[12] P. Courtine and E. Bordes, Appl. Catal., A **157**, 45 (1997).
[13] P. Blaha, K. Schwarz, G. K. H. Madsen, D. Kvasnicka, and J. Luitz, WIEN2K, An Augmented Plane Wave + Local Orbitals Program for Calculating Crystal Properties (Karlheinz Schwarz, Technische Universität Wien, Wein, Austria), 2001. ISBN 3-9501031-1-2.
[14] C. Hébert-Souche, P.-H. Louf, P. Blaha, M. Nelhiebel, J. Luitz, P. Schattschneider, K. Schwarz, and B. Jouffrey, Ultramicroscopy **83**, 9 (2000).
[15] J.P. Perdew, S. Burke, and M. Ernzerhof, Phys. Rev. Lett. **77**, 3865 (1996).
[16] D.S. Su, M. Willinger, C. Hébert-Souche, and R. Schlögl, Micron **34**, 227 (2003).
[17] C. Hébert, M. Willinger, D.S. Su, P. Pongratz, P. Schattschneider, and R. Schlögl, Eur. Phys. J. B **28**, 407 (2002).
[18] R.D. Leapman and L.A. Grunes, Phys. Rev. Lett. **45**, 397 (1980).
[19] J. Fink, Th. Müller-Heinzerling, B. Scheerer, W. Speier, F.U. Hillebrecht, J.C. Fuggle, J. Zaanen, and G.A. Sawatzky, Phys. Rev. B **32**, 4899 (1985).
[20] D.S. Su, M. Wieske, E. Beckmann, A. Blume, G. Mestl, and R. Schlögl, Catal. Lett. **75**, 81 (2001).
[21] F.M.F. de Groot, J. Electron Spectrosc. Relat. Phenom. **15**, 529 (1994).